DEPARTMENT OF CHEMICAL SCIENCES
COLLEGE OF SCIENCES
OLD DOMINION UNIVERSITY
NORFOLK, VIRGINIA 23529

## GAS PERMEATION MEASUREMENTS ON SMALL POLYMER SPECIMENS

By

Karen S. Burns

John D. Van Norman, Principal Investigator

Final Report
For the period ended December 31, 1987

Prepared for the
National Aeronautics and Space Administration
Langley Research Center
Hampton, Virginia 23665

Under
Master Contract Agreement NAS1-17993
Task Authorization No. 59
Dr. George M. Wood, Jr., Technical Monitor
IRD-General Research Instrumentation Branch

February 1988

DEPARTMENT OF CHEMICAL SCIENCES
COLLEGE OF SCIENCES
OLD DOMINION UNIVERSITY
NORFOLK, VIRGINIA 23529


GAS PERMEATION MEASUREMENTS ON
SMALL POLYMER SPECIMENS


By


Karen S. Burns

John D. Van Norman, Principal Investigator


Final Report
For the period ended December 31, 1987

February 1988

# GAS PERMEATION MEASUREMENTS ON
# SMALL POLYMER SPECIMENS

By

Karen S. Burns[1] and John D. Van Norman[2]

## ABSTRACT

Mass spectrometry was used to measure oxygen and nitrogen permeabilities while polarography was used to measure oxygen permeabilities for several contact lens materials. Applicable sample holders were designed and fabricated to accommodate curved and flat specimens with surface areas of 0.5 $cm^2$ and 1.0 $cm^2$ and thicknesses between 0.025 mm and 0.500 mm. A prepared standard was used to calibrate the mass spectrometric analyses.

The oxygen permeability values determined by mass spectrometry were significantly greater than those determined by polarography. This was attributed to the phase boundary phenomena and the limiting oxygen permeance of water inherent in the polarographic technique. Polarographic values determined in this work were in good agreement with proprietary values obtained by polarography, with the exception of one material. Initial efforts to calibrate the methodologies with a Standard Reference Material 1470 from the National Bureau of Standards could not be accomplished due to the extremely low oxygen and nitrogen permeance of the standard and the experimental constraints.

---

[1]Graduate Research Assistant, Old Dominion University, Norfolk, Virginia 23529.
[2]Professor, Old Dominion University, Norfolk, Virginia 23529.

TABLE OF CONTENTS

# LIST OF TABLES

# LIST OF FIGURES

# CHAPTER I

## INTRODUCTION

Man has modified natural polymers for centuries.
Natural polymers include proteins, natural rubber, tar,
gums, and resins. Cellulose is the primary constituent of
wood fibers and cotton but when Celluloid or nitrocellulose
was introduced in 1870 by J. W. and I. S. Hyatt, few would
have foreseen the value of plastics (1). Celluloid has been
used to manufacture brushes, combs, photographic film, glue
fibers, lacquers, and automobile safety glass. In 1908
Baekeland first introduced the totally synthetic plastic
Bakelite which has become the standard for telephone
receivers, electrical insulators, and cooking utensil
handles (1). Properties of plastics such as ease of
fabrication, low cost tooling or molding, low material and
production cost, low density, and high resistance to
corrosion have made them significant materials.

Today, synthetic polymers are used extensively in the
food packaging and building material industries. These
polymers have replaced glass wherever safety and no toxicity
problems are assured.

In 1938 Mullen and Obrig developed the first all
plastic, polymethylmethacrylate contact lens that replaced
glass corneal lenses (2). Since then other polymers have

been developed to satisfy the needs of the ophthalmic industry. In recent years the contact lens industry has developed extended wear contact lens materials which are claimed to transmit oxygen gas at a rate sufficient for corneal metabolic needs to prevent the occurrence of corneal edema (2). The latter requires adaptation of a reliable analytical methodology for evaluating oxygen permeability in small polymeric specimens since these materials are cross-linked polymers and cannot be cast in thin films.

Gas permeability also has an important role in the food packaging and beverage industry. Both the control of bacterial growth and the control of fermentation require application of techniques used to evaluate permeability of oxygen and other gases. These techniques often utilize methods applicable to large sample specimens, but many process control applications will benefit significantly from the improved small sample measurement techniques described here. Additionally, commercial gas producers utilize polymer membrane materials for separation or enrichment processes, and selectively permeable membranes are used for blood gas sampling as well as other medical applications.

Permeability is a physical property of a material which varies for different gases and temperature. It is represented mathematically as the product of diffusivity of the diffusing substance (D) and its Henry's Law solubility (k) in the material (3). Permeability or Dk units used by the contact lens industry are $(cm^2/sec)(ml\ O_2/cm^3 \cdot mm\ Hg)$.

Permeance or transmissibility is Dk/L and is defined as the rate of a gas that permeates through a known area and a known thickness per unit time (3).

Historically, several analytical techniques have been used to determine oxygen content in gases and liquids. As early as 1925, Heyrovsky demonstrated the use of the polarographic electrode to measure dissolved oxygen in saline solution, and by 1940 modified platinum and silver electrodes were used for measurement of partial pressures of oxygen or tension in living tissues (4).

Eustache and Jacquot determined gas permeability of relatively thick specimens by mass spectrometry (5). This work in the 1960's was conducted using polyvinyl chloride (PVC) wine bottles whose nominal surface area was 55 $cm^2$. In the early 1970's, Roper (6) and Gerritse (7) studied the permeability of Teflon (PTFE), PVC, polyethylene and nylon meter length tubing using a gas chromatograph with a thermal conductivity detector. In 1984, Yamamoto, Sakata, and Hirai measured gas permeability values for composite membranes of hexamethyldisiloxane, 1-hexene, and cyclohexene prepared by plasma polymerization (8). Their methodology also utilized thermal conductivity gas chromatography.

Research conducted on packaging materials has made extensive use of spectrophotometric techniques to measure oxygen solubility and oxygen permeability of polymeric materials (9,10,11). These techniques, however, usually require a photosensitive dye to be incorporated within the

polymeric matrix, a method not entirely conducive to many existing polymerization procedures. Additionally, electron spin resonance (ESR) studies on the oxidative process in polyethylene were carried out by Hori et al (12). These data were computer analyzed based on diffusion controlled process theory to determine the diffusion constant (D) and the solubility constant (k) for oxygen.

Fatt, however, made extensive use of the polarographic oxygen sensor method for measuring oxygen permeability in plastic contact lens specimens. He and others have studied oxygen transmissibility (Dk/L) of various materials including polymethylmethacrylate, polyhydroxyethylmetha-crylate, polysiloxanes and composites thereof (13,14,15). Fatt stated there was "no a priori way" of knowing the area of the cathode with any accuracy (14). Therefore, several assumptions in evaluating the electrode area were made using the work of Goldstick (16) and Friedman (17). Fatt evaluated the Dk value for a specimen of agar gel and found the value consistent with what would be expected using Friedman's arguments, but without solubility or diffusion data for oxygen in agar gel.

In 1979 the National Bureau of Standards (NBS) made available a Primary Standard Reference Material SRM-1470 which is well characterized and established (18). SRM-1470, a poly(ethyleneterephthalate) film is a polyester film for certified He, $O_2$, $CO_2$, and $N_2$ gas transmission measurements. The American Society for Testing and Materials standard

test method ASTM:D 1434-75M (19), a manometric determination, was used to establish the gas transmission properties of SRM-1470. This reference material has also been used with ASTM:D 1434-75V (19), a volumetric method, and ASTM:D 3985-81 (19), a coulometric method. Each aforementioned ASTM technique requires a test specimen with a nominal area of 50 sq cm and by design, requires that the test specimen function as a barrier between two gas phase chambers, one side of which is used to measure the gas transmission rate from the other chamber.

## Statement of Problem

The goals of this research were to develop analytical methodologies applicable to the measurement of gas permeabilities on small polymer specimens. Mass spectrometric permeability measurements were advantageous since any permeable gas could be analyzed. Polarography is a very sensitive method for measuring the oxygen content in liquids and has been used extensively for contact lens permeation measurements. Little research has been conducted in verifying the applicability of Standard Reference Material 1470 as a standard for calibration methods used for evaluation of gas permeability in small test specimens. As a result of the relatively low permeability of the SRM-1470 and the small size of contact lenses, it was necessary to utilize the more sensitive methods of mass spectrometry and the more routinely used polarographic technique for oxygen permeation measurements.

CHAPTER II

EXPERIMENTAL

## Apparatus and Materials

All mass spectrometric measurements were made on a
Dupont CEC 21-104 12.7 cm radius magnetic sector mass
spectrometer of the Dempster type using a stainless steel
capillary inlet for continuous introduction of gaseous
samples. The metered capillary inlet was 0.010 inch id,
within which was inserted a 0.008 inch diameter stainless
chromium-nickel alloy wire. The gold leak to the ion source
chamber had a five pinhole pattern over a 32 $mm^2$ area and
samples 0.04% of flow by. The exit slit was set at 0.050
inch to provide a flat top peak.

The electron multiplier detector was a Channeltron
(model 4735) powered by a Fluke 415B power supply operated
at 1000 V direct current. Subsequently, the ion current was
amplified with a Nuclide model EAH-300 pre-amp and measured
with a Nuclide model EA10A electrometer. The resultant
signal was recorded on a Hewlett-Packard 7047A X-Y plotter
as a function of inlet pressure. The inlet pressure was
monitored by a flush diaphragm, unbonded strain gauge
pressure transducer with a range of 0 to 5 psi. It was
powered and amplified by a Pacific Transducer Corporation
SG-100 signal conditioning system. Output pressure was

plotted as the X function of the X-Y plotter recorder.
A schematic diagram of the analysis system is presented in
Figure 1.

Applicable sample holders were designed and fabricated
to accommodate flat specimens as well as contact lenses.
Special precautions were taken to minimize gas volumes yet
optimize transmissibility and thus sensitivity for the small
samples.  Specifications are shown in Figure 2.

In order to eliminate a pressure gradient, a gas flow
system was designed to assure nearly identical gas flow
rates on both sides of the membrane.  A diffusion controlled
concentration gradient through the sample was produced by
passing the analyte gas on one side of the polymer barrier
which allowed the permeating gas to diffuse into the carrier
stream prior to flowing by the mass spectrometer inlet.
Alternately, the impurity analyte in the carrier gas was
determined by utilizing a three-way valve which permitted
the carrier gas to flow on both sides of the membrane.
Argon flow rate was optimized at 4.6 SCCM to enhance signal
and prevent back diffusion of atmospheric gases.
The inlet vacuum was metered to withdraw 0.5 SCCM from the
analysis side of the membrane.  Hastings Raydist controller
(CPR-4P), mass flowmeter valves (CST-100), and an exhaust
flow meter (NALL-100P) were used to regulate flow rates.
Figure 3 presents a schematic diagram of the gas flow
system.

The carrier gas was argon from NASA stock having
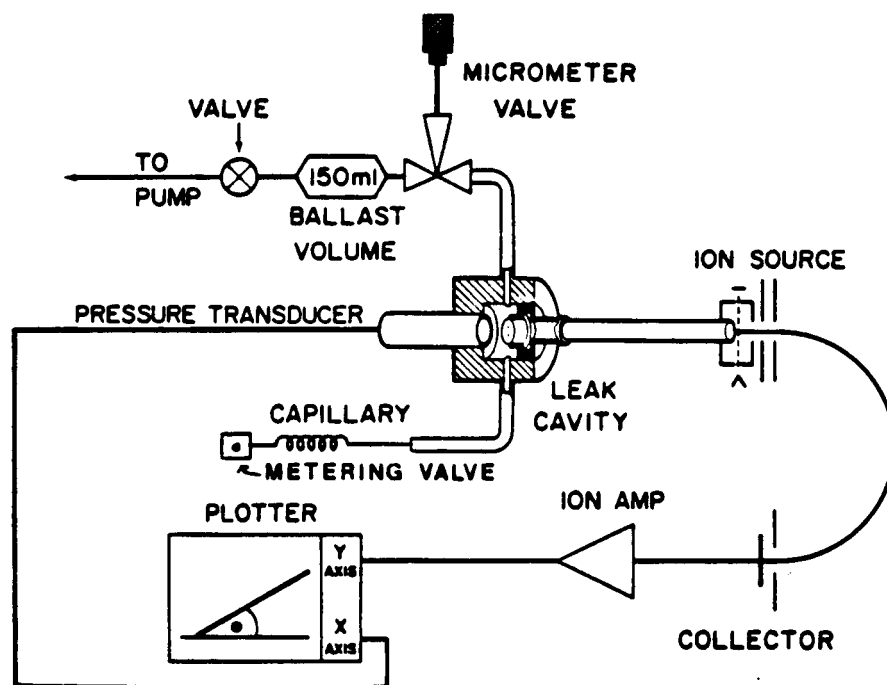
Figure 1.    Schematic Diagram of Mass Spectrometer Analysis
            System.

1/16 Stainless
Steel Tubing

SPECIMEN HOLDER
SCREW CAP (Brass)

30 Threads / Inch

Membrane and
O-ring Seals

Contact Lens Speciman
and O-ring Seal

2.00 mm Inset

8.00 mm
Radius

8.00 mm

OR

9/16 in. Hex

SPECIMEN
HOLDER BASES
(Brass)
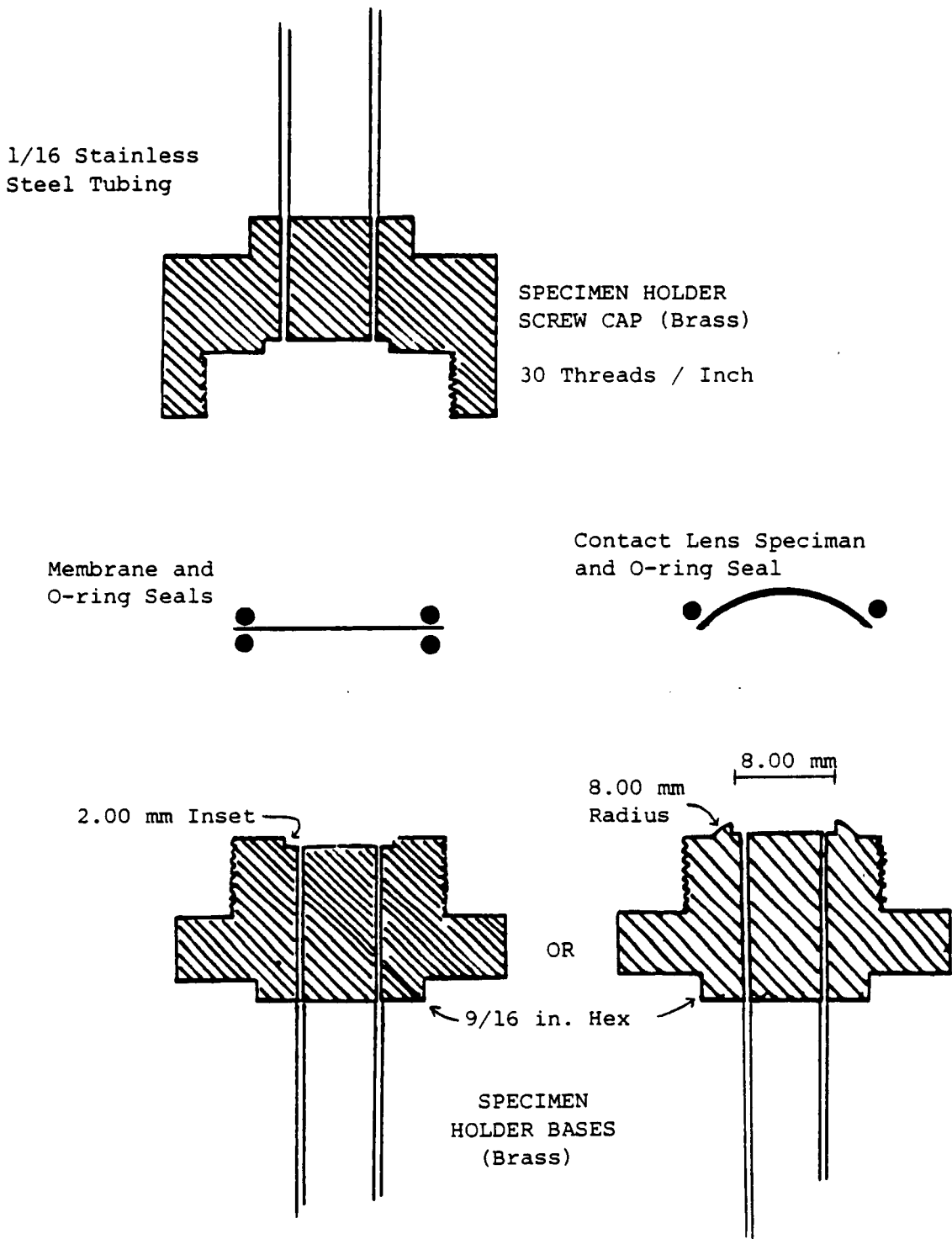
Figure 2.   Mass Spectrometer Sample Holder Accommodating
Flat Specimens and Contact Lens Specimens.
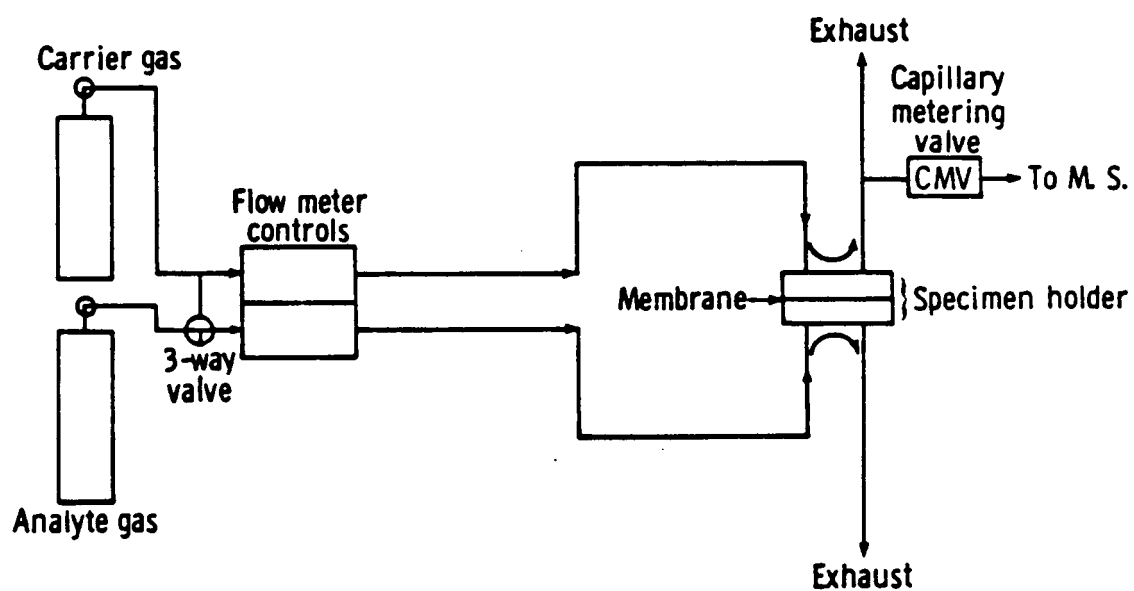
Figure 3.   Gas Flow Schematic for Mass Spectrometric
            Permeation Measurement.

a stated purity of 99.998%. The two analyte gases investigated were nitrogen, also from NASA stock of stated purity 99.998%, and research grade oxygen.

Calibration of the mass spectrometer analysis was accomplished with a prepared standard mixture of air in argon that closely approximated the matrix composition of the permeating mixtures. The standard contained 0.314% $O_2$, 1.17% $N_2$ and 98.52% Argon.

A polarographic oxygen sensing voltammetric cell was designed to accommodate curved and flexible film specimens, and fabricated as shown in Figure 4. The stationary electrode consisted of a gold cathode operated at a constant potential of -0.750 V with respect to the silver plated gold anode. The electrolyte was a 0.1 N NaCl solution. The reduction current was monitored using a PAR 174A Polarographic Analyzer from EK&G Company and recorded on a Tracor FD10A Westronics strip chart recorder. Since the output signal of the analyzer was +10.0 V, the recorder was set to +10.0 V full scale and the current output range scaled accordingly. For the materials analyzed, the maximum recorder response was generally $5\mu A$ or $10\mu A$ at equilibrium. A schematic diagram of the analysis system is presented in Figure 5.

The Standard Reference Material SRM-1470 was purchased from the National Bureau of Standards (NBS). Fifteen sheets of a poly(ethyleneterephthalate) film were supplied. Three samples, 1.35 cm in diameter, were die cut for the mass

Furled Grip

BRASS SCREW·CAP for CELL

Delrin Gasket

Contact Lens Specimen

1/4 in.

1/8 in.

8.00 mm Radius

BRASS SLEEVE

Set Screw

DELRIN BASE

Cathode

0.030 in. Gold Wire Leads

Anode
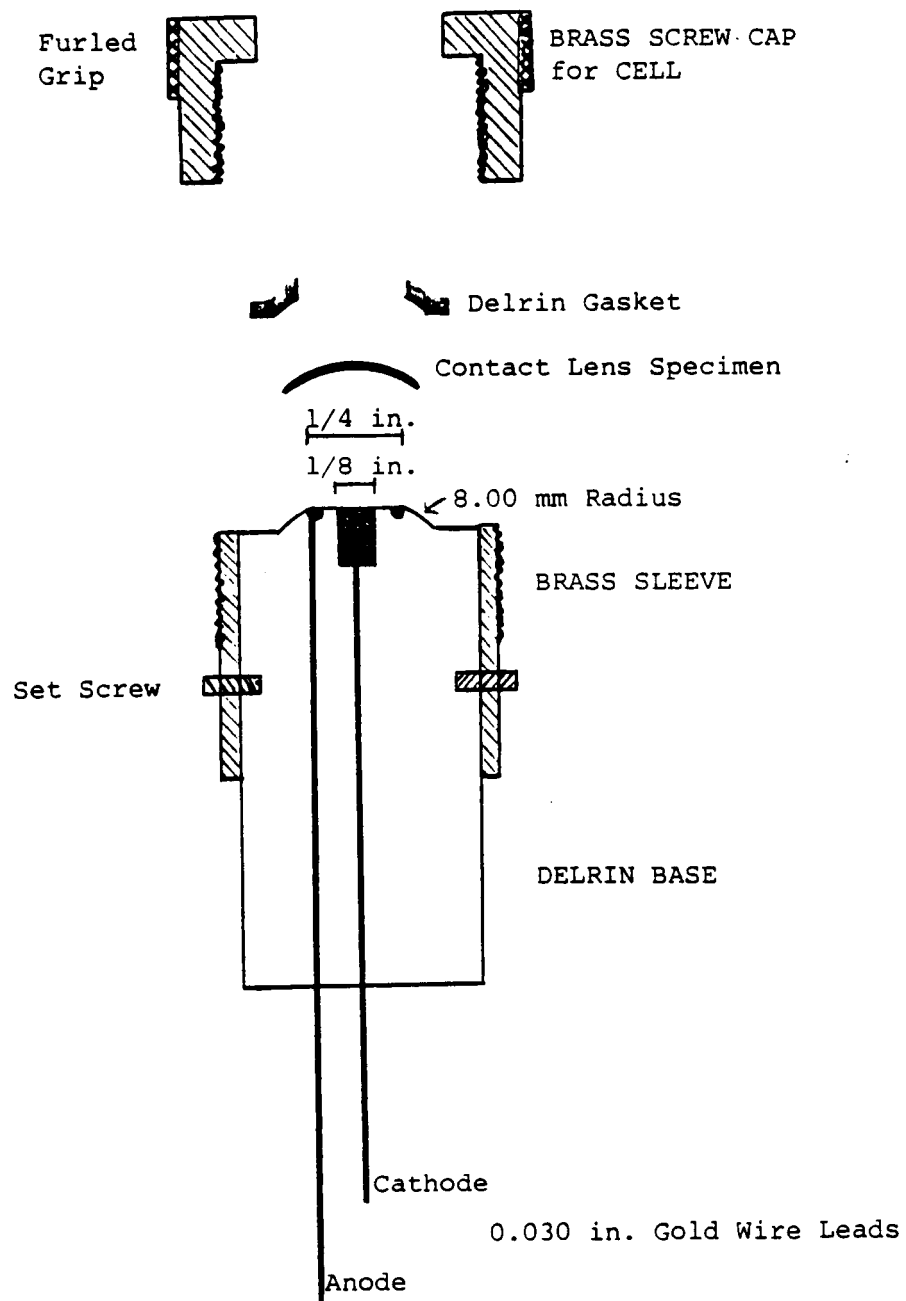
Figure 4.  Oxygen Sensing Voltammetric Cell for Polaro-
graphic Analysis.
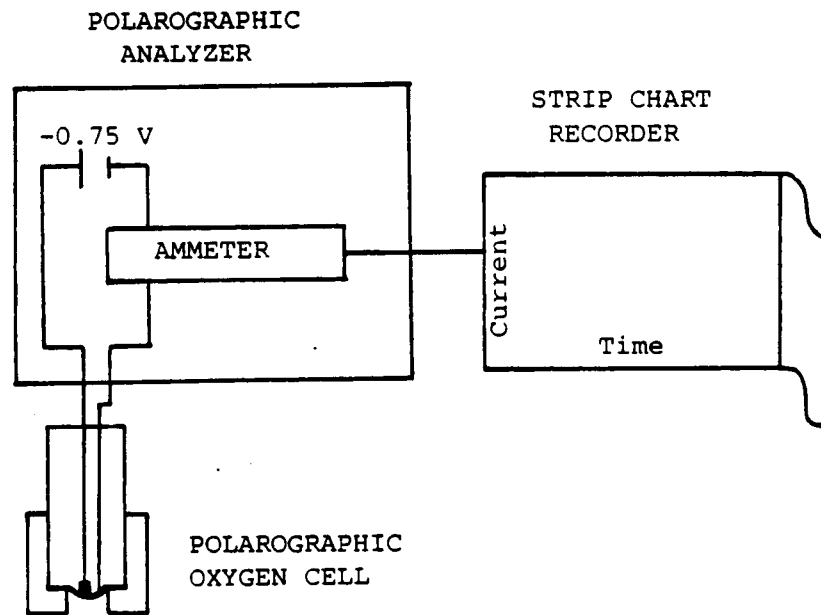
Figure 5. Schematic Diagram of Polarographic Analysis
System.

spectrometer measurements. Each was from a separate sheet and labeled 7a, b, and c. Because smaller specimens were required for the polarographic analysis, four samples were die cut from two additional sheets. These samples were labeled 7A-1, 7A-2, 7B-1, 7B-2 and measured 0.80 cm in diameter. Although the SRM-1470 is certified for permeance values of nitrogen, oxygen, carbon dioxide, and helium, only the appropriate data for nitrogen and oxygen are presented in Table I. The certified values were converted to those units used in reporting permeability of contact lenses. Permeance or transmissibility is Dk/L whereas permeability is Dk; D is the diffusion coefficient, k is the solubility constant from Henry's Law and L is the thickness or path length of the diffusing gas.

The contact lens specimens were manufactured with a concave radius of 8.00 mm with a chord diameter of 10.00 mm. Parallel convex surfaces were cut with a radius of 8.20 mm; therefore, the center thickness (CT) was nominally 0.20 mm. Since specimen thickness is a critical measurement in permeability calculations, the CT of each lens was measured to an accuracy of ± 0.002 mm and reported in the appropriate data table. Figure 6 diagrams the geometry of the contact lens specimen. The samples investigated included two specimens from each of the six materials and are labeled 1 through 6, a and b accordingly. It was not necessary to clean or condition the lenses with soaking or wetting solutions. Conventional hard lens polishing techniques had been used

TABLE I   PERMEABILITY DATA FOR NBS STANDARD REFERENCE
MATERIAL 1470[a]

| QUANTITY | UNIT | OXYGEN | NITROGEN |
|---|---|---|---|
| Permeance[b], 23°C Pg or Dk/L | $\dfrac{pmole}{m^2 \cdot s \cdot mm\ Hg}$ | 0.352 | 0.0421 |
| Permeance[c], 23°C Pg or Dk/L | $\dfrac{ml}{cm^3 \cdot mm\ Hg} \times \dfrac{cm}{s}$ | $1.14 \times 10^{-10}$ | $1.36 \times 10^{-11}$ |
| Thickness, L | cm | $2.34 \times 10^{-3}$ | $2.34 \times 10^{-3}$ |
| Permeability[c], Dk | $\dfrac{ml}{cm^2 \cdot mm\ Hg} \times \dfrac{cm}{s}$ | $2.67 \times 10^{-13}$ | $3.19 \times 10^{-14}$ |
| Temperature Coefficient, Bg | $K^{-1}$ | 0.03762 | 0.05211 |
| Error Coefficient for Mean, Cg | – | 0.014 | 0.023 |
| Error Coefficient for Difference Between Mean and Single Specimen, Kg | – | 0.045 | 0.057 |

a.   (ref. 18)

b.   $Pg(T) = Pg\ (296.15)\,e^{Bg(T-296.15)}$

c.   Expressed in units used by the Contact Lens
     Manufacturers Association

CONVEX or
FRONT SURFACE

Radius = 8.20 mm

CONCAVE or
BASE CURVE

Radius = 8.00 mm

LENS
CENTER
THICKNESS
or CT =
0.20 mm

CHORD DIAMETER or
LENS SIZE = 10.00 mm
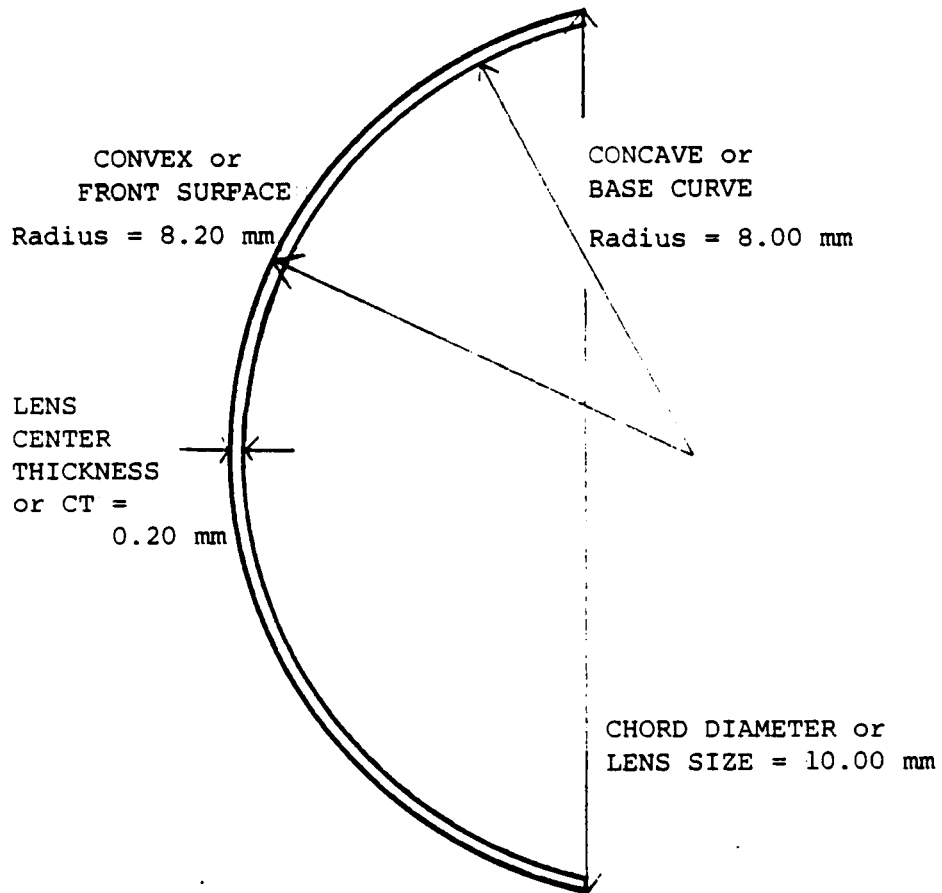
Figure 6.  The Geometry of the Contact Lens Specimen.

to polish the surfaces.

Cigarette papers, SUP-AIR brand from JOB, were used to assist in centering lenses in place while securing specimen holder for polarographic measurements. The papers had over thirty-five perforations per $cm^2$ and assured an electrolyte layer under the film specimens.

## Mass Spectrometer Procedure

Unlike scanning mass spectrometry, which measures the ion current as a function of the mass-to-charge ratio (m/e) at constant pressure, this method monitors ion current as a function of inlet total pressure for a specific ion of the species being analyzed. The procedure is often referred to as the dynamic delta method since it quantitatively relates slope of the ion current vs inlet pressure to analyte concentration (20).

Due to the very low analyte concentration and the inherent detector drift, argon m/e 36 with isotopic abundance 0.334%, was chosen as the internal standard to ratio all analyte species. Oxygen m/e 32 and nitrogen m/e 14 were chosen as the analyte species for measurement of oxygen and nitrogen permeation concentrations. Instrumental parameters for mass spectrometer measurements are presented in Table II.

TABLE II   ELECTRONIC PARAMETERS FOR MASS SPECTROMETER
          MEASUREMENTS

| Instrumental Parameter | $O_2$ Sample | $N_2$ Sample | Argon | $O_2$ Std. Mix | $N_2$ Std. Mix |
|---|---|---|---|---|---|
| Electrometer (V FS) | 30 | 3 | 30 | 30 | 30 |
| Y (Volts/inch) | 0.005 | 0.05 | 0.05 | 0.05 | 0.05 |
| X (Volts/inch) | 0.05 | 0.05 | 0.05 | 0.05 | 0.05 |

A typical analysis run was performed as follows:
(1) the appropriate m/e was focused on the center of its
flat top peak; (2) the electronic parameters were selected;
(3) the inlet pressure was pumped down to less than 0.01
Torr and a mass spectrometer system pressure of approxi-
mately $5.0 \times 10^{-7}$ Torr; (4) the inlet vacuum pump valve was
closed; (5) the inlet capillary metering valve was opened to
obtain the desired flow rate; (6) the slope was recorded
until the inlet pressure produced a system pressure of
approximately $2.0 \times 10^{-5}$ Torr; (7) the inlet vacuum pump
valve was opened; and (8) the inlet capillary metering valve
was closed which allowed the system to pump down for the
next analysis.   Typical dynamic delta data for an oxygen
permeation measurement are shown in Figure 7.

An altered gas flow pattern required a full purge of
approximately 143 SCCM for five to ten minutes followed by
equilibration at 4.6 SCCM for thirty minutes to sixty
minutes for the more permeable materials.   Subsequently, the
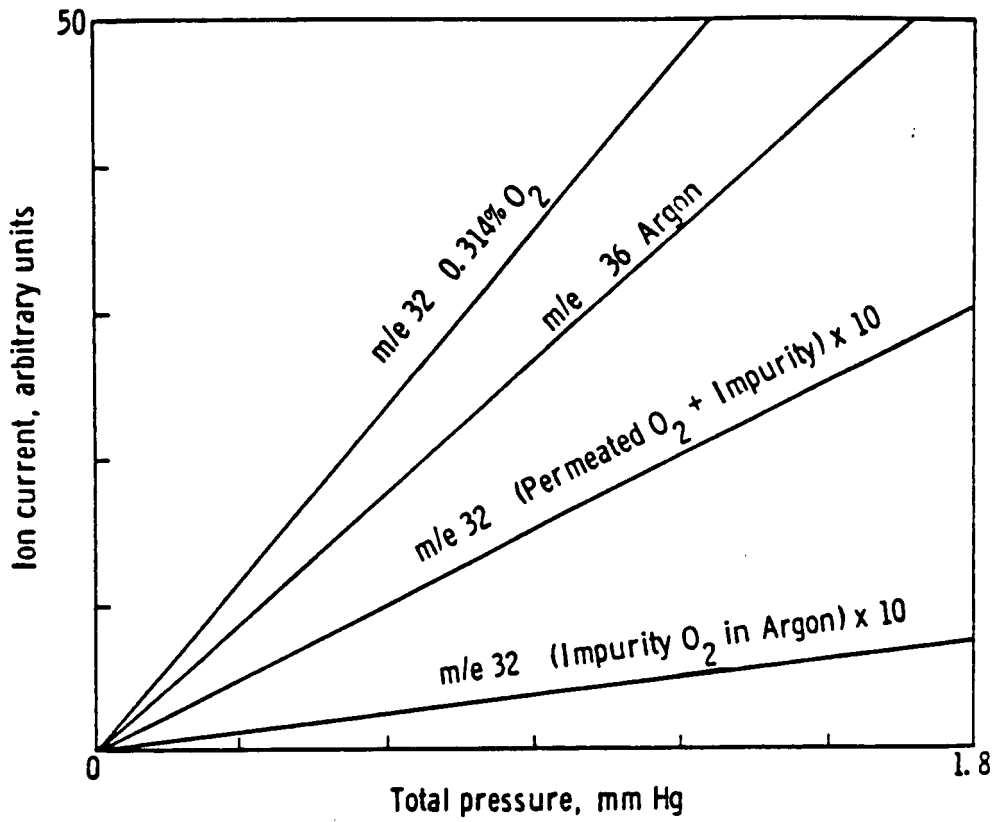
Figure 7.  Typical Dynamic Delta Data for Oxygen Permeation
Measurement.

metered capillary valve was opened to pump out dead volumes for new gas composition measurements.

A permeability data set for each specimen consisted of repetitive runs in which both the analysis runs and carrier gas impurity runs were bracketed with runs of the internal standard. The relative slope ratios are found in Tables III through XVI. All values are for triplicate analyses except for material 7 and 1a where n = 5. The corrected relative slope ratios were obtained by subtracting the impurity relative slope ratio from the total relative slope ratio. Listed values were later corrected for the instrumental parameters of Table II when making calculations of compositions and the resulting permeability values.

Polarographic Procedure

In the polarographic method, the current measured is directly proportional to the amount of oxygen reduced at the cathode. The two half-cell reactions are:

(1) Cathodic :     $O_2 + 2H_2O + 4e^- = 4OH^-$

(2) Anodic    :     $4Cl^- + 4Ag = 4AgCl + 4e^-$
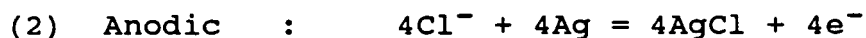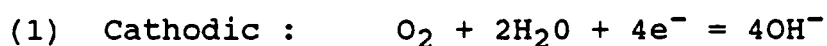
A typical analysis was completed in the following manner. Initially a drop of electrolyte was placed on an electrode surface which was covered with a 1.15 cm diameter disc of cigarette paper. This procedure was utilized by Fatt to assure a uniform electrolyte film under the lens (21). It was necessary to use this with the flat film specimens and, for consistency, was used with the lenses also. Subsequently, a sample was placed over the cigarette

TABLE III   OXYGEN RELATIVE SLOPE RATIOS FOR MATERIAL 1

| Material<br>Code No. | 1a<br>8/28 | 1b<br>9/18 |
|---|---|---|
| $^{36}M_{ref}$ | 0.918<br>± 0.014 | 0.744<br>± 0.027 |
| $^{32}M$<br>Impurity | 0.158<br>± 0.002 | 0.130<br>± 0.002 |
| $^{32}M/^{36}M$<br>Impurity | 0.172<br>± 0.003 | 0.174<br>± 0.007 |
| $^{36}M_{ref}$ | 0.906<br>± 0.004 | 0.694<br>± 0.015 |
| $^{32}M$<br>Total | 0.302<br>± 0.014 | 0.227<br>± 0.003 |
| $^{32}M/^{36}M$<br>Total | 0.333<br>± 0.015 | 0.327<br>± 0.008 |
| $^{32}M/^{36}M$<br>Imp. Cor. | 0.161<br>± 0.015 | 0.153<br>± 0.011 |
| T  (°C) | 21.4 | 22.5 |
| Thickness  (cm) | 0.0182 | 0.0202 |

TABLE IV  OXYGEN RELATIVE SLOPE RATIOS FOR MATERIAL 2

| Material Code No. | 2a 8/31 | 2b 9/3 |
|---|---|---|
| $^{36}M_{ref}$ | 0.886 ± 0.003 | 0.866 ± 0.008 |
| $^{32}M$ Impurity | 0.164 ± 0.001 | 0.150 ± 0.003 |
| $^{32}M/^{36}M$ Impurity | 0.185 ± 0.001 | 0.173 ± 0.004 |
| $^{36}M_{ref}$ | 0.905 ± 0.007 | 0.833 ± 0.016 |
| $^{32}M$ Total | 0.429 ± 0.016 | 0.426 ± 0.005 |
| $^{32}M/^{36}M$ Total | 0.474 ± 0.018 | 0.511 ± 0.011 |
| $^{32}M/^{36}M$ Imp. Cor. | 0.289 ± 0.018 | 0.338 ± 0.012 |
| T (°C) | 21.9 | 21.7 |
| Thickness (cm) | 0.0195 | 0.0187 |

TABLE V   OXYGEN RELATIVE SLOPE RATIOS FOR MATERIAL 3

| Material Code No. | 3a 9/1 | 3b 9/3 |
|---|---|---|
| $^{36}M_{ref}$ | 0.907 ± 0.015 | 0.815 ± 0.012 |
| $^{32}M$ Impurity | 0.165 ± 0.008 | 0.152 ± 0.006 |
| $^{32}M/^{36}M$ Impurity | 0.182 ± 0.009 | 0.186 ± 0.008 |
| $^{36}M_{ref}$ | 0.931 ± 0.012 | 0.821 ± 0.008 |
| $^{32}M$ Total | 0.605 ± 0.008 | 0.543 ± 0.006 |
| $^{32}M/^{36}M$ Total | 0.650 ± 0.012 | 0.661 ± 0.010 |
| $^{32}M/^{36}M$ Imp. Cor. | 0.468 ± 0.015 | 0.475 ± 0.013 |
| T (°C) | 21.7 | 21.7 |
| Thickness (cm) | 0.0177 | 0.0189 |

TABLE VI   OXYGEN RELATIVE SLOPE RATIOS FOR MATERIAL 4

| Material Code No. | 4a 9/8 | 4b 9/4 |
|---|---|---|
| $^{36}M_{ref}$ | 0.868 ± 0.011 | 0.820 ± 0.016 |
| $^{32}M$ Impurity | 0.176 ± 0.005 | 0.161 ± 0.006 |
| $^{32}M/^{36}M$ Impurity | 0.203 ± 0.004 | 0.196 ± 0.008 |
| $^{36}M_{ref}$ | 0.894 ± 0.021 | 0.839 ± 0.013 |
| $^{32}M$ Total | 0.744 ± 0.001 | 0.765 ± 0.004 |
| $^{32}M/^{36}M$ Total | 0.832 ± 0.019 | 0.912 ± 0.014 |
| $^{32}M/^{36}M$ Imp. Cor. | 0.629 ± 0.019 | 0.716 ± 0.016 |
| T (°C) | 20.7 | 22.4 |
| Thickness (cm) | 0.0189 | 0.0197 |

TABLE VII   OXYGEN RELATIVE SLOPE RATIOS FOR MATERIAL 5

| Material<br>Code No. | 5a<br>9/10 | 5b<br>9/11 |
|---|---|---|
| $^{36}M_{ref}$ | 0.750<br>± 0.003 | 0.771<br>± 0.015 |
| $^{32}M$<br>Impurity | 0.147<br>± 0.004 | 0.154<br>± 0.009 |
| $^{32}M/^{36}M$<br>Impurity | 0.196<br>± 0.005 | 0.200<br>± 0.012 |
| $^{36}M_{ref}$ | 0.753<br>± 0.006 | 0.751<br>± 0.006 |
| $^{32}M$<br>Total | 0.428<br>± 0.007 | 0.372<br>± 0.005 |
| $^{32}M/^{36}M$<br>Total | 0.569<br>± 0.010 | 0.495<br>± 0.008 |
| $^{32}M/^{36}M$<br>Imp. Cor. | 0.373<br>± 0.011 | 0.295<br>± 0.014 |
| T  (°C) | 21.7 | 22.2 |
| Thickness (cm) | 0.0186 | 0.0192 |

TABLE VIII   OXYGEN RELATIVE SLOPE RATIOS FOR MATERIAL 6

| Material Code No. | 6a 9/22 | 6b 9/28 | 6c 10/1 |
|---|---|---|---|
| $^{36}M_{ref}$ | 0.716 ± 0.014 | 0.838 ± 0.014 | 0.761 ± 0.003 |
| $^{32}M$ Impurity | 0.137 ± 0.003 | 0.174 ± 0.006 | 0.0693 ± 0.0052 |
| $^{32}M/^{36}M$ Impurity | 0.191 ± 0.006 | 0.208 ± 0.008 | 0.0911 ± 0.0068 |
| $^{36}M_{ref}$ | 0.723 ± 0.008 | 0.860 ± 0.016 | 0.777 ± 0.007 |
| $^{32}M$ Total | 0.189 ± 0.003 | 0.225 ± 0.002 | 0.0946 ± 0.0023 |
| $^{32}M/^{36}M$ Total | 0.261 ± 0.005 | 0.262 ± 0.006 | 0.122 ± 0.003 |
| $^{32}M/^{36}M$ Imp. Cor. | 0.070 ± 0.008 | 0.054 ± 0.010 | 0.031 ± 0.008 |
| T (°C) | 22.5 | 22.2 | 19.7 |
| Thickness (cm) | 0.0211 | 0.0211 | 0.0207 |

TABLE IX   OXYGEN RELATIVE SLOPE RATIOS FOR MATERIAL 7,
SRM - 1470

| Material Code | 7a 8/23 | 7a 9/14 | 7c 9/15 | 7a 9/21 |
|---|---|---|---|---|
| $^{36}M_{ref}$ | 1.08 ± 0.07 | 0.722 ± 0.018 | 0.716 ± 0.005 | 0.731 ± 0.014 |
| $^{32}M$ Impurity | 0.142 ± 0.005 | 0.144 ± 0.009 | 0.136 ± 0.008 | 0.140 ± 0.002 |
| $^{32}M/^{36}M$ Impurity | 0.131 ± 0.010 | 0.199 ± 0.013 | 0.190 ± 0.011 | 0.192 ± 0.005 |
| $^{36}M_{ref}$ | 1.17 ± 0.02 | 0.752 ± 0.021 | 0.735 ± 0.010 | 0.709 ± 0.004 |
| $^{32}M$ Total | 0.209 ± 0.004 | 0.186 ± 0.004 | 0.168 ± 0.006 | 0.186 ± 0.003 |
| $^{32}M/^{36}M$ Total | 0.179 ± 0.005 | 0.247 ± 0.009 | 0.228 ± 0.009 | 0.262 ± 0.004 |
| $^{32}M/^{36}M$ Imp. Cor. | 0.048 ± 0.010 | 0.048 ± 0.016 | 0.038 ± 0.014 | 0.070 ± 0.006 |
| T (°C) | 20.0 | 22.2 | 21.0 | 23.0 |
| Thickness (cm) | $2.34\times10^{-3}$ | $2.34\times10^{-3}$ | $2.34\times10^{-3}$ | $2.34\times10^{-3}$ |

TABLE X   NITROGEN RELATIVE SLOPE RATIOS FOR MATERIAL 1

| Material Code | 1a 8/28 | 1a 10/6 | 1b 9/18 | 1b 10/6 |
|---|---|---|---|---|
| $^{36}M_{ref}$ | 0.993 ± 0.028 | 0.726 ± 0.010 | 0.686 ± 0.004 | 0.735 ± 0.010 |
| $^{14}M$ Impurity | 0.0683 ± 0.0044 | 0.0538 ± 0.0031 | 0.0651 ± 0.0017 | 0.0491 ± 0.0014 |
| $^{14}M/^{36}M$ Impurity | 0.0687 ± 0.0048 | 0.0741 ± 0.0044 | 0.0949 ± 0.0026 | 0.0668 ± 0.0021 |
| $^{36}M_{ref}$ | 0.957 ± 0.017 | 0.718 ± 0.010 | 0.689 ± 0.008 | 0.728 ± 0.004 |
| $^{14}M$ Total | 0.113 ± 0.006 | 0.0911 ± 0.0034 | 0.0996 ± 0.0012 | 0.0785 ± 0.0024 |
| $^{14}M/^{36}M$ Total | 0.118 ± 0.007 | 0.127 ± 0.005 | 0.1445 ± 0.0024 | 0.108 ± 0.003 |
| $^{14}M/^{36}M$ Imp. Cor. | 0.0495 ± 0.0085 | 0.0529 ± 0.0067 | 0.0496 ± 0.0035 | 0.0412 ± 0.0037 |
| T (°C) | 21.1 | 21.7 | 22.2 | 20.6 |
| Thickness (cm) | 0.0182 | 0.0182 | 0.0202 | 0.0202 |

TABLE XI  NITROGEN RELATIVE RATIOS FOR MATERIAL 2

| Material Code No. | 2a 8/31 | 2b 9/3 |
|---|---|---|
| $^{36}M_{ref}$ | 0.974 ± 0.022 | 0.902 ± 0.013 |
| $^{14}M$ Impurity | 0.0696 ± 0.0027 | 0.0620 ± 0.0029 |
| $^{14}M/^{36}M$ Impurity | 0.0714 ± 0.0032 | 0.0687 ± 0.0034 |
| $^{36}M_{ref}$ | 0.950 ± 0.006 | 0.944 ± 0.045 |
| $^{14}M$ Total | 0.112 ± 0.016 | 0.122 ± 0.004 |
| $^{14}M/^{36}M$ Total | 0.118 ± 0.017 | 0.129 ± 0.008 |
| $^{14}M/^{36}M$ Imp. Cor. | 0.0470 ± 0.017 | 0.0608 ± 0.0087 |
| T (°C) | 21.7 | 21.3 |
| Thickness (cm) | 0.0195 | 0.0187 |

TABLE XII   NITROGEN RELATIVE SLOPE RATIOS FOR MATERIAL 3

| Material Code No. | 3a 9/2 | 3b 9/4 |
|---|---|---|
| $^{36}M_{ref}$ | 0.916 ± 0.009 | 0.832 ± 0.006 |
| $^{14}M$ Impurity | 0.0569 ± 0.0017 | 0.0491 ± 0.0033 |
| $^{14}M/^{36}M$ Impurity | 0.0621 ± 0.0020 | 0.0590 ± 0.0040 |
| $^{36}M_{ref}$ | 0.891 ± 0.004 | 0.928 ± 0.013 |
| $^{14}M$ Total | 0.127 ± 0.010 | 0.135 ± 0.004 |
| $^{14}M/^{36}M$ Total | 0.142 ± 0.011 | 0.146 ± 0.005 |
| $^{14}M/^{36}M$ Imp. Cor. | 0.0805 ± 0.011 | 0.0870 ± 0.0064 |
| T (°C) | 20.6 | 20.0 |
| Thickness (cm) | 0.0177 | 0.0189 |

TABLE XIII   NITROGEN RELATIVE SLOPE RATIOS FOR MATERIAL 4

| Material Code No. | 4a 9/8 | 4b 9/9 |
|---|---|---|
| $^{36}M_{ref}$ | 0.802 ± 0.002 | 0.752 ± 0.004 |
| $^{14}M$ Impurity | 0.0540 ± 0.0012 | 0.0560 ± 0.0027 |
| $^{14}M/^{36}M$ Impurity | 0.0673 ± 0.0015 | 0.0744 ± 0.0036 |
| $^{36}M_{ref}$ | 0.818 ± 0.002 | 0.775 ± 0.006 |
| $^{14}M$ Total | 0.202 ± 0.007 | 0.174 ± 0.004 |
| $^{14}M/^{36}M$ Total | 0.247 ± 0.009 | 0.224 ± 0.005 |
| $^{14}M/^{36}M$ Imp. Cor. | 0.180 ± 0.009 | 0.150 ± 0.006 |
| T (°C) | 22.2 | 21.1 |
| Thickness (cm) | 0.0189 | 0.0197 |

TABLE XIV   NITROGEN RELATIVE SLOPE RATIOS FOR MATERIAL 5

| Material Code No. | 5a 9/10 | 5b 9/11 |
|---|---|---|
| $^{36}M_{ref}$ | 0.781 ± 0.008 | 0.741 ± 0.016 |
| $^{14}M$ Impurity | 0.0600 ± 0.0029 | 0.0496 ± 0.0014 |
| $^{14}M/^{36}M$ Impurity | 0.0768 ± 0.0038 | 0.0669 ± 0.0024 |
| $^{36}M_{ref}$ | 0.776 ± 0.002 | 0.739 ± 0.001 |
| $^{14}M$ Total | 0.144 ± 0.002 | 0.105 ± 0.002 |
| $^{14}M/^{36}M$ Total | 0.186 ± 0.003 | 0.142 ± 0.003 |
| $^{14}M/^{36}M$ Imp. Cor. | 0.109 ± 0.005 | 0.0753 ± 0.0038 |
| T (°C) | 21.3 | 21.7 |
| Thickness (cm) | 0.0186 | 0.0192 |

TABLE XV  NITROGEN RELATIVE SLOPE RATIOS FOR MATERIAL 6

| Material Code No. | 6a 9/25 | 6b 10/1 |
|---|---|---|
| $^{36}M_{ref}$ | 0.795 ± 0.008 | 0.735 ± 0.012 |
| $^{14}M$ Impurity | 0.0480 ± 0.0013 | 0.0918 ± 0.0034 |
| $^{14}M/^{36}M$ Impurity | 0.0604 ± 0.0017 | 0.125 ± 0.005 |
| $^{36}M_{ref}$ | 0.764 ± 0.011 | 0.745 ± 0.004 |
| $^{14}M$ Total | 0.0838 ± 0.0038 | 0.127 ± 0.002 |
| $^{14}M/^{36}M$ Total | 0.110 ± 0.005 | 0.1713 ± 0.0028 |
| $^{14}M/^{36}M$ Imp. Cor. | 0.0496 ± 0.0018 | 0.0463 ± 0.0058 |
| T (°C) | 21.7 | 22.2 |
| Thickness (cm) | 0.0211 | 0.0207 |

TABLE XVI   NITROGEN RELATIVE SLOPE RATIOS FOR MATERIAL 7,
SRM - 1470

| Material Code No. | 7a 8/25 | 7b 8/14 | 7c 8/15 |
|---|---|---|---|
| $^{36}M_{ref}$ | 1.05 ± 0.02 | 0.785 ± 0.015 | 0.704 ± 0.015 |
| $^{14}M$ Impurity | 0.0549 ± 0.0057 | 0.0500 ± 0.0031 | 0.0477 ± 0.0048 |
| $^{14}M/^{36}M$ Impurity | 0.0524 ± 0.0052 | 0.0637 ± 0.0041 | 0.0678 ± 0.0070 |
| $^{36}M_{ref}$ | 1.08 ± 0.07 | 0.768 ± 0.012 | 0.712 ± 0.007 |
| $^{14}M$ Total | 0.0939 ± 0.0036 | 0.0733 ± 0.0041 | 0.0768 ± 0.0007 |
| $^{14}M/^{36}M$ Total | 0.0872 ± 0.0065 | 0.0954 ± 0.0055 | 0.1078 ± 0.0015 |
| $^{14}M/^{36}M$ Imp. Cor. | 0.0348 ± 0.0083 | 0.0317 ± 0.0068 | 0.0400 ± 0.0072 |
| T (°C) | 22.2 | 21.7 | 21.9 |
| Thickness (cm) | $2.34 \times 10^{-3}$ | $2.34 \times 10^{-3}$ | $2.34 \times 10^{-3}$ |

paper with additional electrolyte such that no air pockets under the specimen were visible. The Delrin gasket and screw cap sealed the sample securely. Alternately, the current was monitored as a function of time for both residual and permeating oxygen until equilibrium was established when current response was constant. The residual dark current was established by submerging the cell into nitrogen deaerated deionized water. The cell was removed and the excess water wiped off the membrane surface. Total current including residual current as well as the reduction current of permeating atmospheric oxygen was then monitored at room temperature. Periodically, the silver chloride was dissolved from the anode with 3 M $NH_3$. Typical current measurements are shown in Figure 8.

Unlike the mass spectrometric analysis, only one lens from each material was analyzed with duplicate measurements. Three of the SRM-1470 specimens were analyzed; however, the magnitude of permeating current was indistinguishable from residual cell currents as a result of the low permeation rates. Consequently, these data are not included in Table XVII, Polarographic Current Measurements. The table also includes other pertinent lens data for permeation calculations.
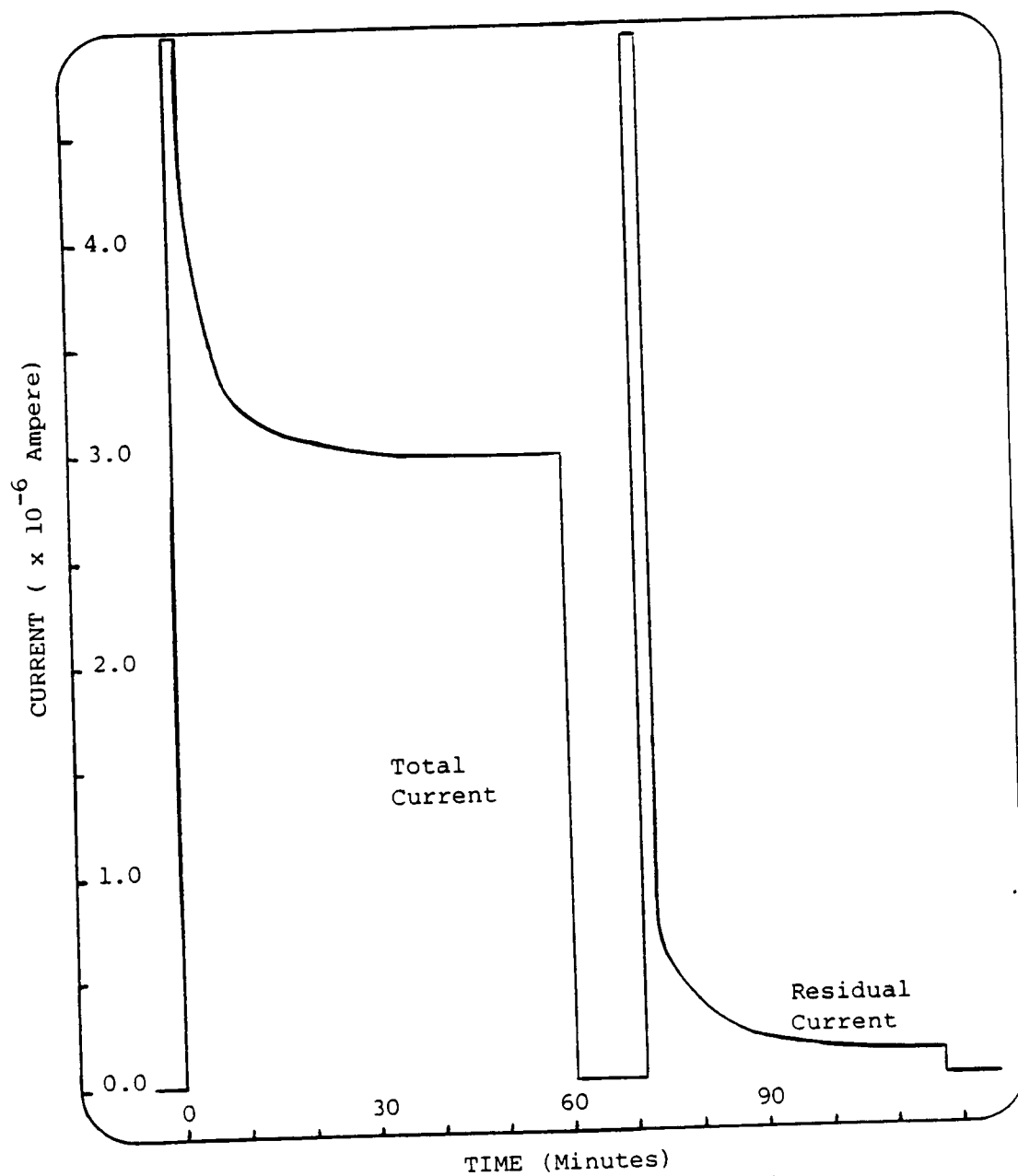
Figure 8. Typical Polarographic Data for Current Measure-
ments.

TABLE XVII   POLAROGRAPHIC CURRENT MEASUREMENTS FOR CONTACT
LENS SPECIMENS

| Material Code No. | $i_{TOTAL}$ $\times 10^{-6}$A | $i_{RESIDUAL}$ $\times 10^{-6}$A | $i_{RED.}$ $\times 10^{-6}$A | Thickness L (cm) | T (°C) |
|---|---|---|---|---|---|
| 1a | 1.54 ±0.01 | 0.14 ±0.05 | 1.40 ±0.05 | 0.0182 | 26 |
| 2a | 2.48 ±0.11 | 0.24 ±0.01 | 2.24 ±0.11 | 0.0195 | 27 |
| 3a[1] | 2.69 ±0.06 | 0.18 ±0.02 | 2.51 ±0.06 | 0.0177 | 25 |
| b[2] | 2.62 | 0.17 | 2.45 | 0.0189 | 26 |
| 4a[1] | 2.98 ±0.06 | 0.47 ±0.09 | 2.51 ±0.10 | 0.0189 | 28 |
| b[1] | 3.28 ±0.04 | 0.26 ±0.01 | 3.02 ±0.05 | 0.0197 | 24 |
| 5a | 2.42 ±0.04 | 0.16 ±0.01 | 2.26 ±0.04 | 0.0186 | 26 |
| 6a | 0.38 ±0.03 | 0.15 ±0.03 | 0.23 ±0.04 | 0.0211 | 27 |

1.  Triplicate analysis

2.  Single analysis

# CHAPTER III

## RESULTS

### Mass Spectrometric Calculations

In mass spectrometry the intensity of peak or ion current is directly proportional to its component partial pressure or concentration in the sample. When the ion current is measured as a function of total pressure the slope or dynamic delta function can be represented as

$$\text{mol \% A} = \frac{P_A}{P_T} \times 100 = k_A \frac{i_A}{P_T} \times 100 = k_A' \frac{\triangle y}{\triangle x} \times 100$$

Where    mol % is also Vol % or concentration

$P_A$ is the partial pressure of a particular analyte

$P_T$ is the total pressure

$i_A$ is the ion current of A

$\triangle y/\triangle x$ is the slope

$k_A'$ is the proportionality constant for the analysis

When mol % A is the standard mix concentration of either oxygen or nitrogen and is ratioed to the mol % Argon in the standard mix, a relative proportionality constant, $K_A'$, can be determined for each analyte using argon as the internal reference.

The determination of the relative proportionality constant for the oxygen analyses follows:

$$K'_{O_2} = \frac{k'_{O_2}}{k'_{Ar}} = \frac{\% \ O_2 \text{ std mix } / \text{ slope } O_2 \text{ std mix}}{\% \ Ar \text{ std mix } / \text{ slope } Ar \text{ std mix}}$$

$$= \frac{0.314\% \ O_2 \ / \ \dfrac{8.75 \text{ in}}{7.36 \text{ in}} \times \dfrac{0.05 \text{ V/in}}{0.05 \text{ V/in}}}{98.52\% \ Ar \ / \ \dfrac{10.00 \text{ in}}{11.35 \text{ in}} \times \dfrac{0.05 \text{ V/in}}{0.05 \text{ V/in}}}$$

$$= 0.00243 \ \frac{\% \ O_2 \ / \text{ slope units } O_2}{\% \ Ar \ / \text{ slope units } Ar} \qquad \text{or}$$

$$= 0.00243 \ (\% \ O_2 \cdot SUAr) \ / \ \% \ Ar \cdot SUO_2$$

Relative slope units for the standard mix were obtained from data in Appendix A.

Subsequent substitution of $K'_{O_2}$ to solve for mol % $O_2$ that has permeated a particular membrane can be readily accomplished. Assuming that the % $O_2$ permeating the membrane is insignificant compared to the % Ar then

$$\text{mol } \% \ O_2 = K'_{O_2} \cdot \text{Relative Corrected Slope} \cdot \% \ Ar$$

which becomes

$$\text{mol } \% \ O_2 = K'_{O_2} \cdot \text{Relative Corrected Slope} \cdot 100\% \ Ar$$

Gas permeance, Dk/L, of a material is defined as

$$Dk/L = \frac{\text{Gas diffusivity x Henry's Law Constant}}{\text{Specimen thickness}}$$

The permeance of a gas through a material may be experimentally determined by measuring the permeant gas concentration in the argon carrier gas flowing past the

opposite side of a specimen which is exposed to a pure analyte gas A on one side as follows:

$$Dk/L = \frac{\text{Mole fraction A x Flow rate Ar}}{\text{Specimen area x Pressure Applied x Specimen thickness}}$$

Subsequently, permeability or Dk was determined using the equation

$$Dk = \frac{(\% \; O_2) \; ml \; O_2}{100 \; ml \; Ar} \cdot \frac{4.6 \; ml \; Ar}{min} \cdot \frac{1 \; min}{60 \; sec} \cdot \frac{thickness}{Area \cdot 760 \; mm \; Hg}$$

where the specimen area was 0.538 $cm^2$ for the lenses and 1.13 $cm^2$ for SRM-1470, the thickness in cm was taken from appropriate measurement data in Tables III through IX, and % $O_2$ was calculated from appropriate impurity corrected relative slope data from Tables III through IX and recorder attenuation factors from Table II. Results of oxygen permeability calculations for the contact lens and SRM 1470 specimens are reported in Table XVIII.

The relative proportionality constant for nitrogen, $K'_{N_2}$, was similarly calculated and determined to be

$$0.00421 \; (\%N_2 \cdot SUAr)/(\%Ar \cdot SUN_2).$$

Nitrogen permeability was likewise calculated using the appropriate data from Tables X through XVI in addition to recorder and electrometer attenuation factors from Table II. These results are reported in Table XIX.

TABLE XVIII    OXYGEN PERMEABILITY FOR CONTACT LENS AND
                SRM-1470 SPECIMENS ANALYZED BY MASS
                SPECTROMETRY[a]

| Material Code No. | Permeability or Dk $\frac{ml\ O_2}{cm^3\ \cdot\ mm\ Hg}\ \cdot\ \frac{cm^2}{s}$ | Temperature °C |
|---|---|---|
| 1a | $13.3 \pm 1.2 \times 10^{-11}$ | 21.4 |
| b | $14.0 \pm 1.0 \times 10^{-11}$ | 22.5 |
| 2a | $25.6 \pm 1.6 \times 10^{-11}$ | 21.9 |
| b | $28.6 \pm 1.0 \times 10^{-11}$ | 21.7 |
| 3a | $37.5 \pm 1.1 \times 10^{-11}$ | 21.7 |
| b | $40.6 \pm 1.1 \times 10^{-11}$ | 21.7 |
| 4a | $53.9 \pm 1.6 \times 10^{-11}$ | 20.7 |
| b | $63.9 \pm 1.4 \times 10^{-11}$ | 22.4 |
| 5a | $31.5 \pm 0.8 \times 10^{-11}$ | 21.7 |
| b | $25.7 \pm 1.1 \times 10^{-11}$ | 22.2 |
| 6a (9/22) | $6.69 \pm 0.74 \times 10^{-11}$ | 22.5 |
| a (9/28) | $5.15 \pm 0.96 \times 10^{-11}$ | 22.2 |
| b | $2.90 \pm 0.74 \times 10^{-11}$ | 19.7 |
| 7a (8/23) | $0.349 \pm 0.072 \times 10^{-11}$ | 23.0 |
| a (9/21) | $0.340 \pm 0.030 \times 10^{-11}$ | 23.0 |
| b | $0.280 \pm 0.090 \times 10^{-11}$ | 23.0 |
| c | $0.279 \pm 0.102 \times 10^{-11}$ | 23.0 |

a.  Values for Material 7 are indicative of impurity level
    oxygen and not permeating oxygen.

TABLE XIX    NITROGEN PERMEABILITY FOR CONTACT LENS AND
             SRM-1470 SPECIMENS ANALYZED BY MASS
             SPECTROMETRY[a]

| Material Code No. | Permeability or Dk $\dfrac{ml\ N_2}{cm^3 \cdot mm\ Hg} \cdot \dfrac{cm^2}{s}$ | Temperature °C |
|---|---|---|
| 1a (8/28) | $7.08 \pm 1.22 \times 10^{-11}$ | 21.1 |
| a (10/6) | $7.56 \pm 0.96 \times 10^{-11}$ | 21.7 |
| b (9/18) | $7.86 \pm 0.56 \times 10^{-11}$ | 22.2 |
| b (10/6) | $6.51 \pm 0.59 \times 10^{-11}$ | 20.6 |
| 2a | $7.19 \pm 2.60 \times 10^{-11}$ | 21.7 |
| b | $8.92 \pm 1.27 \times 10^{-11}$ | 21.3 |
| 3a | $11.2 \pm 1.5 \times 10^{-11}$ | 20.6 |
| b | $12.9 \pm 0.9 \times 10^{-11}$ | 20.0 |
| 4a | $26.7 \pm 1.3 \times 10^{-11}$ | 22.2 |
| b | $23.2 \pm 0.8 \times 10^{-11}$ | 21.1 |
| 5a | $15.9 \pm 0.7 \times 10^{-11}$ | 21.3 |
| b | $11.4 \pm 0.6 \times 10^{-11}$ | 21.7 |
| 6a | $8.22 \pm 0.30 \times 10^{-11}$ | 21.7 |
| b | $7.54 \pm 0.94 \times 10^{-11}$ | 22.2 |
| 7a | $0.335 \pm 0.080 \times 10^{-11}$ | 23.0 |
| b | $0.337 \pm 0.073 \times 10^{-11}$ | 23.0 |
| c | $0.405 \pm 0.073 \times 10^{-11}$ | 23.0 |

a.  Values for Material 7 are indicative of impurity level
    nitrogen and not permeating nitrogen.

## Polarographic Calculations

Polarographic oxygen permeability determinations for contact lens and film type materials are well documented in the literature (13-15, 21-25). When the test specimen is placed directly on a polarographic oxygen sensor (POS), permeability calculations assume that the volume between the sensor and the test specimen is negligible, and the rate of oxygen diffusing through a test specimen is equal to the rate of oxygen being consumed by the electrode. Thus the method combines Fick's First Law of Diffusion and Faraday Law into the following equation for calculation of permeance from which permeability or Dk/L can be determined (14):

$$Dk/L = \frac{i\text{-}i\ residual}{NAFP_{O_2}} \qquad and$$

$$Dk = \frac{L\ (i\text{-}i\ residual)}{NAFP_{O_2}}$$

where
| | | |
|---|---|---|
| D | = | Diffusion coefficient |
| k | = | solubility constant from Henry's Law |
| L | = | thickness of specimen (cm) |
| N | = | 4, the number of electron moles necessary to reduce one mole of oxygen |
| A | = | electrode area, 0.079 $cm^2$ |
| F | = | Faraday constant, 96,487 coulombs per equivalent or amp $sec^{-1}$ per mole electrons |
| $P_{O_2}$ | = | partial pressure of oxygen on free side of test specimen, assuming dry standard atmosphere, 155 mm Hg at 20°C. |
| i-i residual | = | reduction current measured experimentally by subtracting cell current from total current, Table XVII. |

Table XX reports permeability results for six contact lens

TABLE XX    OXYGEN PERMEABILITY OF CONTACT LENS SPECIMENS
ANALYZED BY POLAROGRAPHY

| Material Code No. | Permeability or Dk $\dfrac{ml\ O_2}{cm^3 \cdot mm\ Hg} \cdot \dfrac{cm^2}{s}$ | Temperature °C |
|---|---|---|
| 1a | $12.1 \pm 0.4 \times 10^{-11}$ | 26 |
| 2a | $20.7 \pm 0.1 \times 10^{-11}$ | 27 |
| 3a | $21.0 \pm 0.5 \times 10^{-11}$ | 25 |
| b | $21.9 \quad\quad \times 10^{-11}$ | 26 |
| 4a | $22.4 \pm 0.9 \times 10^{-11}$ | 28 |
| b | $27.0 \pm 0.4 \times 10^{-11}$ | 24 |
| 5a | $19.9 \pm 0.4 \times 10^{-11}$ | 26 |
| 6a | $2.3 \pm 0.4 \times 10^{-11}$ | 27 |

materials.  All values are for n = 2, except for material

3a, 4a and b where n = 3 and material 3b where n = 1.

## Discussion

The permeability of a gas through a membrane is a

temperature dependent property and all measurements in this

work were obtained under measured ambient temperature

conditions.  The mass spectrometric oxygen permeability

results are significantly greater than proprietary values

which were obtained polarographically.  Polarographic

results obtained in this work were comparable to proprietary

values with the exception of one material.  Table XXI

compares the results for oxygen permeabilities obtained by

the two methodologies.  It is widely accepted that silicone

or fluorocarbon copolymers in polymer matrices tend to

increase oxygen permeability.  However, as a result of their

hydrophobic nature, they may exhibit boundary layer resis-

tance to diffusive flow in a gas-membrane-water (dissolved

oxygen) interface where a gas-membrane-gas interface would

not demonstrate this phenomenon (22-25).  Unlike other

polarographic studies, in this work the electrode design had

a 0.67 mm distance between the cathode and the concave or

base curve surface of the lens.  Fatt stated that this

distance must be less than 0.20 mm to prevent mixing and

assure a diffusion controlled process; should mixing occur,

the resulting measured permeability values would be too

large (14).  The polarographic oxygen permeability values

are smaller and not larger than those obtained by mass

TABLE XXI   COMPARATIVE RESULTS FOR OXYGEN PERMEABILITY
            MEASURED BY MASS SPECTROMETRIC AND POLAROGRAPHIC
            METHODS

| Oxygen Permeability or Dk x $10^{-11}$ ml $O_2$/cm $\cdot$ s $\cdot$ mm Hg | | | | | |
|---|---|---|---|---|---|
| **Mass Spectrometry** | | (°C) | **Polarography** | | (°C) |
| 1a | 13.3 ± 1.2 | (21.4) | 1a | 12.1 ± 0.4 | (26) |
| b | 14.0 ± 1.0 | (22.5) | | | |
| 2a | 25.6 ± 1.6 | (21.9) | 2a | 20.7 ± 0.1 | (27) |
| b | 28.6 ± 1.0 | (21.7) | | | |
| 3a | 37.5 ± 1.1 | (21.7) | 3a | 21.0 ± 0.5 | (25) |
| b | 40.6 ± 1.1 | (21.7) | b | 21.9 | (26) |
| 4a | 53.9 ± 1.6 | (20.7) | 4a | 22.4 ± 0.9 | (28) |
| b | 63.9 ± 1.4 | (22.4) | b | ·27.0 ± 0.4 | (24) |
| 5a | 31.5 ± 0.8 | (21.7) | 5a | 19.9 ± 0.4 | (26) |
| b | 25.7 ± 1.1 | (22.2) | | | |
| 6a | 5.92 ± 0.87 | (22.4) | 6a | 2.3 ± 0.4 | (27) |
| b | 2.90 ± 0.74 | (19.7) | | | |

spectrometry. This observation, at least in part, may be explained by the boundary layer phenomenon.

In comparing nitrogen and oxygen permeabilities measured by mass spectrometry, it is notable that only material 6 had greater nitrogen permeance than oxygen permeance. Gerritse reported that among the many materials tested by gas chromatography, only nylon exhibited this phenomenon (7).

The certified SRM-1470 permeance values for both oxygen and nitrogen are eight-fold less than that determined mass spectrometrically. Under the experimental conditions it was also determined oxygen m/e 32 impurity was 45 ppm compared to the 2 ppm the membrane was expected to permeate, and nitrogen m/e 14 impurity was 30 ppm compared to less than 1 ppm the membrane was anticipated to permeate. Consequently, the low permeability of the SRM-1470 could not be measured accurately, and a standard mixture was subsequently used to calibrate the instrument for subsequent gas analyses. Additionally, the mass spectrometrically measured oxygen and nitrogen permeabilities are within variance of the same value. It would be a remote possibility that all the SRM-1470 specimens had pin hole leaks. Again, the more plausible interpretation would be that the amount of impurity oxygen and nitrogen was much larger than that permeating the membrane.

In the polarographic method, the low permeability of the SRM-1470 also prevented its use as a calibration

standard for the electrode area. With a known permeance or Dk/L and a discernable reduction current, it would be possible to calculate an effective electrode area with a greater accuracy than one calculated geometrically.

CHAPTER IV

CONCLUSION

The research conducted demonstrated that the perme-
ability of the NBS Standard Reference material 1470 was too
low to allow its use as a standard for calibration of the
mass spectrometer or the polarograph under the specimen size
and temperature condition constraints of the experiment.
However, it is possible that a good software program in
conjunction with improved signal processing methods and
greater argon purity may allow the use of the SRM-1470 as
a standard for calibration for mass spectrometrically deter-
mined permeabilities.

Inasmuch as polarographically measured oxygen perme-
ability can exhibit immobile boundary resistance in a
diffusion controlled process, it should also be pointed out
that the oxygen permeability of water solutions approximates
$79 \times 10^{-11}$ ml $O_2$/cm· s · mm Hg at 37° C (26). This suggests
that·materials with greater oxygen permeability than water
cannot be determined by the polarographic method. Thus, the
mass spectrometry method with a gas-membrane-gas interface
should more accurately represents a true gas permeability as
described by the definition of the physical property Dk.

One method of evaluating the limiting permeance of
water would be to use a material with a known Dk of 400 or

higher and evaluate the polarographically determined value. This experiment should be performed with an electrode whose surface more closely conforms to the surface of the membrane such that mixing does not occur. Additionally, the material must not exhibit a boundary layer. A boundary layer would be verified if a differing permeability value were measured for a gas-membrane-liquid interface than for a liquid-membrane-liquid interface. The liquid-membrane-liquid interface could be obtained by submerging the polarographic oxygen sensor in an oxygen saturated water solution which has a known partial pressure at a specific temperature.

The ability to correlate the temperature related permeability data accurately requires that a temperature coefficient be determined for each material. Permeance values could be determined at various temperatures under controlled conditions. A plot of log permeability versus inverse temperature would produce a slope whose value is the temperature coefficient. Future research in this area would also enable the evaluation of materials for applications at various temperatures.

Mass spectrometry could be utilized to determine carbon dioxide permeabilities. Carbon dioxide has an important role in many metabolic processes. Additionally gas chromatography and Fourier transform infrared spectrometry (FTIR) could be used to study permeability processes. Of special interest would be gas permeabilities analyzed by FTIR since the membrane structure could be studied while gases were

dissolved with its polymer matrix.  FTIR techniques also permit analysis of surface structure which could assist in interpretation of boundary layer diffusion processes and surface characteristics such as wettability.

BIBLIOGRAPHY

Reference

1. Driver, W. E.; <u>Plastics Chemistry and Technology</u>; Van Nostrand Reinhold Company; New York, 1979; Chapter 1.

2. Lowther, G. E.; <u>Contact Lenses:  Procedures and Techniques</u>; Butterworths; Woburn, MA, 1982.

3. "Standard Reference Materials:  SRM 1470; Polyester Film for Oxygen Gas Transmission Measurements"; <u>NBS Spec. Publ.</u> (U.S.) June, 1979, No. 260-58.

4. Clark, L. C.  In <u>Polarographic Oxygen Sensors</u>; Fatt, I., CRC Press; Cleveland, Ohio, 1976.

5. Eustache, H.; Jacquot, P.  "Determining gas permeability of thick plastic films by mass spectrometry", <u>Modern Plastics</u>, 1968, 45(10), pp 163-164, 169-170, 172.

6. Roper, F. G.  "Some effects of the permeability of P.T.F.E. gas sample loops used in gas chromatography", <u>J. of Chrom. Sci.</u>, Vol. 9, November 1971, pp. 697-699.

7. Gerritse, R. G.  "Gas chromatographic measurement of the permeability of PTFE, PVC, polyethylene and nylon tubing towards oxygen and nitrogen", <u>J. of Chrom.</u>, Vol. 77, 1973, pp. 406-409.

8. Yamamoto, M.; Sakata, J.; Hirai, M.  "Plasma polymerized membrane and gas permeability. I." <u>J. of Appl. Polym. Sci.</u>, Vol. 29, 1984, pp 2981-2987.

9. Shaw. G.  "Quenching by oxygen diffusion of phosphorescence emission of aromatic molecules in polymethyl methacrylate", <u>Trans. Faraday Soc.</u>, Vol. 63, No. 9, 1967, pp 2181-2189.

10. Petrak, K.  "Permeability of oxygen through polymers. I.  A novel spectrophotochemical method", <u>J. of Appl. Polym. Sci.</u>, Vol. 23, 1979, pp 2365-2371.

11. Rooney, M. L.; Holland, R. V.  "Singlet $O_2$, an intermediate in the inhibition of oxygen permeation through polymer films", <u>Chemistry and Industry (London)</u>, No. 24, 1979, pp 900-901.

    Rooney, M. L.; Holland, R. V.  "Measuring oxygen permeability of polymer films by a new singlet oxygen technique", <u>Angew. Makromol. Chem.</u>, Vol. 88, 1980, pp 209-221.
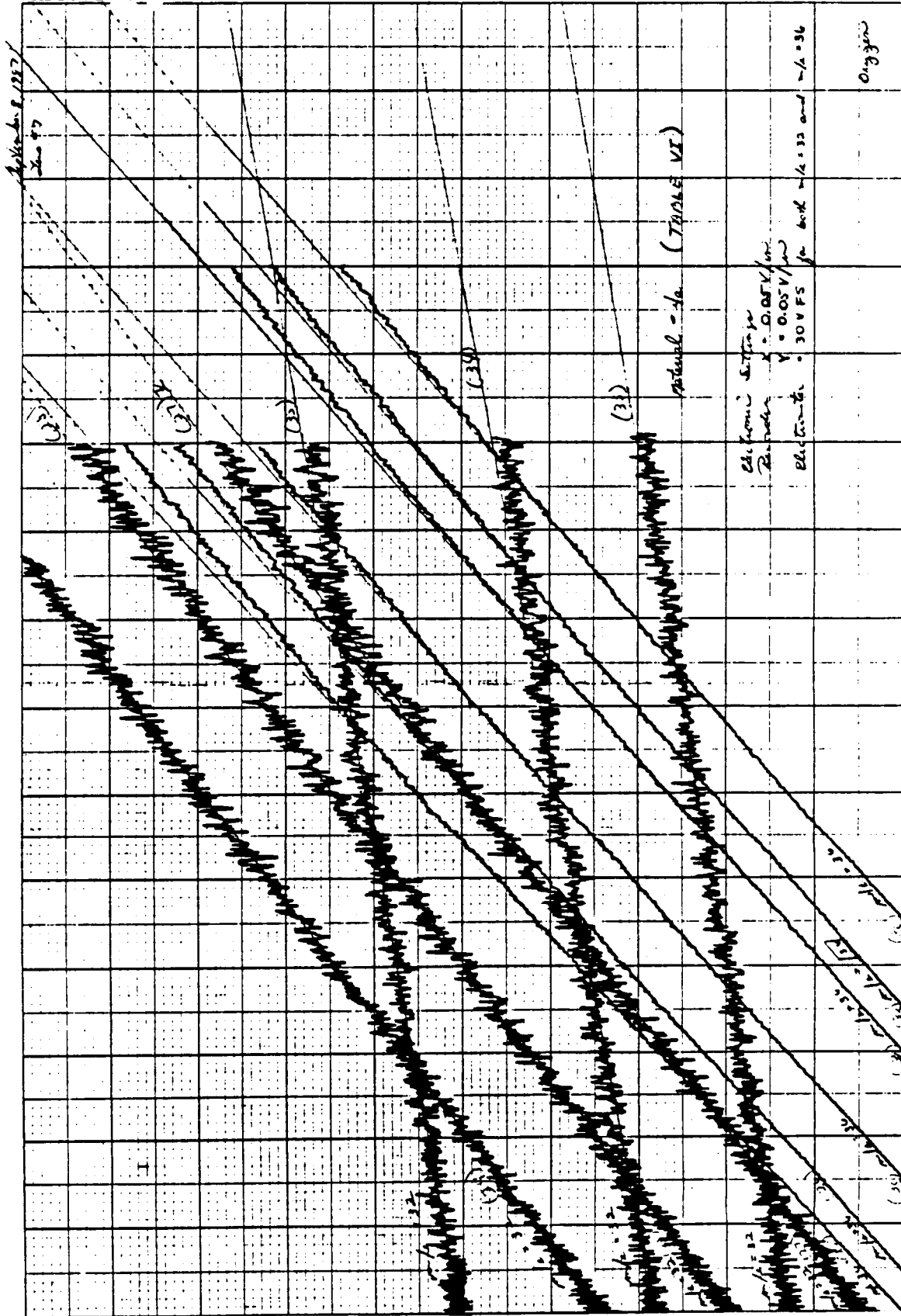
12. Hori, Y.; Shimada, S.; Kashiwabara, H. "E.s.r. studies on oxidation processes in irradiated polyethylene: 1. Diffusion of oxygen into amorphous parts at low temperatures", Polymer, Vol. 18, Feb. 1977, pp 151-154.

    Hori, Y.; Shimada, S.; Kashiwabara, H. "E.s.r. studies on oxidative processes in irradiated polyethylene: 2. Diffusion of oxygen into crystalline regions", Polymer, Vol. 20, Feb. 1979, pp 181-186.

13. Hamano, H.; Kawabe, H.; Mitsunage, S. "Reproducible measurement of oxygen permeability (Dk) of contact lens materials", CLAO J., Vol. 11, No. 3, July 1985, pp 221-226.

14. Fatt, I.; St. Helen, R. "Oxygen tension under an oxygen permeable contact lens", Am. J. Optom. and Arch. Am. Acad. Optom., Vol. 48, No. 7, 1971, pp 545-555.

15. Yang, W.; Smolen V. F.; Peppas, N. A. "Oxygen permeability coefficients of polymers for hard and soft lens applications", J. of Membrane Sci., Vol. 9, 1981, pp 53-67.

16. Goldstick, T. K. "Diffusion of oxygen in protein solutions", Ph.D. thesis, University of California, Berkeley, 1966.

17. Friedman, L. "Structure of agar gels from studies of diffusion", J. Am. Chem. Soc., Vol. 52 (4), 1930, pp 1311-1314.

18. Barnes, J. D. "National Bureau of Standards Certificate, Standard Reference Material 1470, Polyester Plastic Film for Gas Transmission", Office of Standard Reference Materials, Washington, D.C., February, 1982.

19. Annual Book of ASTM Standards, Part 35; ASTM: Philadelphia, 1981.

20. Hughes, D. B.; Nowlin, T. D. "Trace gas analysis", Presented at the 19th Annual Conference on Mass Spectrometry and Allied Topics, Atlanta, Georgia, 1971.

21. Fatt, I. Oxygen Transmissibility and the Permeability of Gas Permeable Hard Contact Lenses and Materials", Int. CL Clinic, 1984, Vol. II, No. 3, pp 175-186.

22. Hwang, S. T., Tang, T. E. S.; Kammermeyer, K. "Transport of dissolved oxygen through silicone rubber membrane", J. Macromolecular Science, Physical Ed., B5(1): 1-10, 1971.

23. Yasuda, H.; Lamaze, C. E. "Transfer of gas to dissolved oxygen in water via porous and nonporous polymer membranes", _J. Applied Poly, Science_, 16;597-601, 1972.

24. Yasuda, H.; Peterlin, A. "Diffusive and bulk flow transport in polymers", _J. Applied Poly, Science_, 17;433-442.

25. Hwang, S. T.; Kammermeyer, K. "Effect of thickness on permeability", _Polymer Science and Technology - Vol. 6: Permeability of Plastic Films and Coatings to Gases, Vapors, and Liquids_; New York: Plenum Press, 1974, pp 197-205.

26. Baumgartl, H.; Lubbers, D. W. In _Polarographic Oxygen Sensors_; Gnaiger, E.; Forstner, H., Eds.; Spring-Valag Berlin Heidelberg, New York, 1983; p. 57.
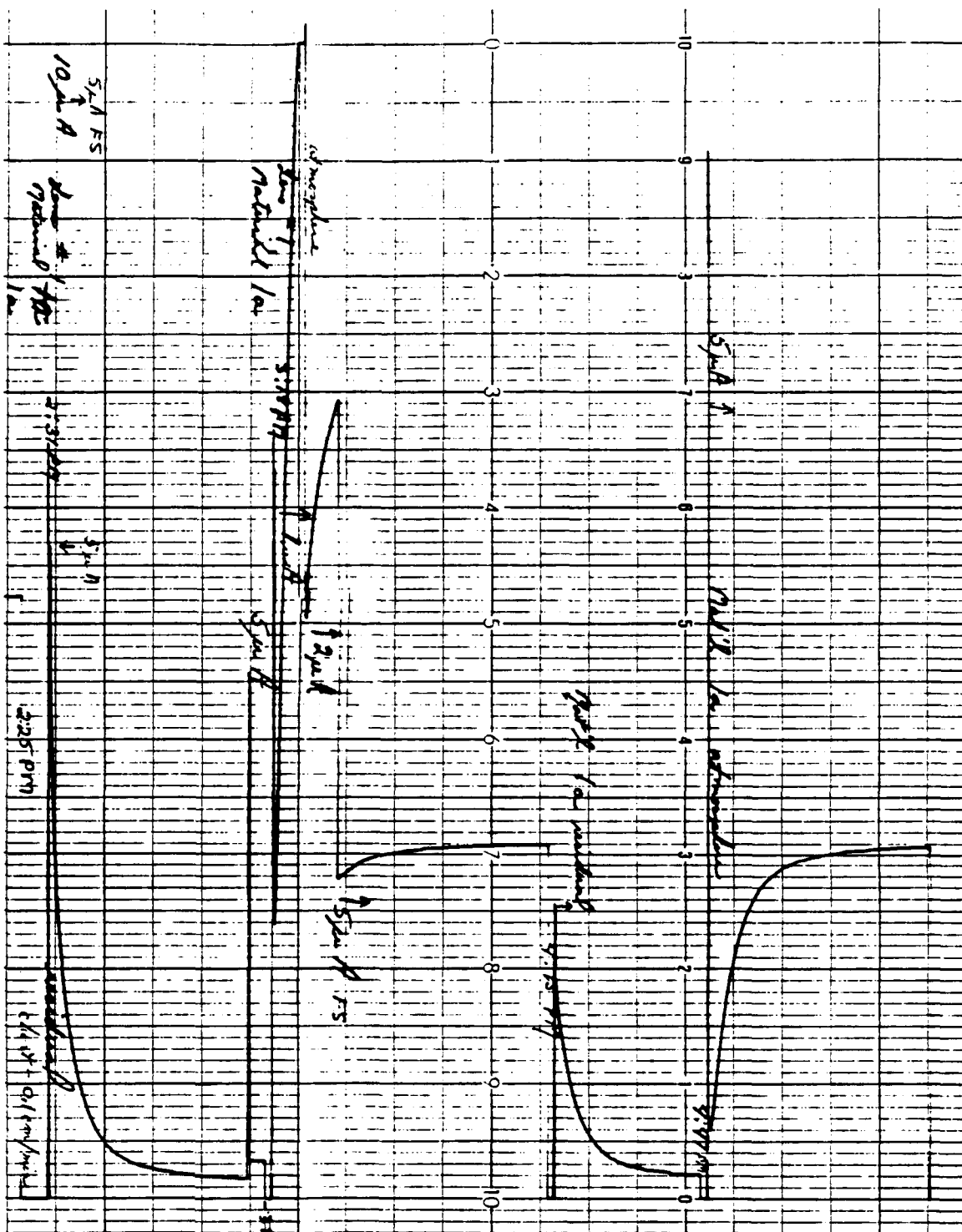
APPENDICES

APPENDIX A

APPENDIX A

APPENDIX B

APPENDIX C

APPENDIX C